Chemical Control of Highly Porous Silica Xerogels: Physical Properties and Morphology

Alexandra Fidalgo,[†] M. Emília Rosa,[‡] and Laura M. Ilharco*[,†]

Centro de Química-Física Molecular, Complexo I, Instituto Superior Técnico, Av. Rovisco Pais 1, 1049-001 Lisboa, Portugal, and ICEMS (Instituto de Ciência e Engenharia de Materiais e Superfícies), Departamento de Engenharia de Materiais, Instituto Superior Técnico, Av. Rovisco Pais 1, 1049-001 Lisboa, Portugal

Received January 13, 2003. Revised Manuscript Received March 13, 2003

Highly porous silica xerogels were synthesized by the sol−gel process under atmospheric conditions. The silica alcogels were prepared by a two-step acid/base-catalyzed hydrolysis/condensation of tetraethoxysilane (TEOS), with a water:TEOS molar ratio of 4, in 2-propanol. The catalysts used in the two steps were HCl and NH_3, respectively, and the catalytic conditions were varied by changing the molar ratios HCl/TEOS (in the first step) and NH_3/HCl (in the second step). After aging in an appropriate solution, the alcogels were washed and subcritically dried from 2-propanol, under atmospheric pressure. The resulting silica xerogels were characterized by the volume shrinkage upon drying, envelope density determinations, scanning electron microscopy, and nitrogen sorption isotherms. It is shown that by chemical control of the hydrolysis and condensation steps, through pH variation only, it is possible to obtain monolithic materials with properties similar to aerogels, stable under atmospheric conditions. Densities as low as 0.37 g cm^{-3}, corresponding to porosities of 80%, were obtained for xerogels with specific surface areas of ∼940 m^2 g^{-1} and a bimodal pore structure, with a narrow mesopore size distribution (average pore diameter of 8 nm).

1. Introduction

The fields of application of highly porous silica xerogels broaden continuously, as the production costs are reduced and the properties improved, mostly due to modifications in the synthesis processes.[1−3] Independent from specific requirements, some properties are acknowledged as fundamental, such as the stiffness and strength of the gel network (that will prevent cracking and reduce shrinkage upon drying) and the endurance to the working environment (that will ensure a good long-term performance). The network strength and stiffness are essentially determined by the aging of the wet gel.[4,5] The long-term performance under atmospheric conditions depends on avoiding moisture condensation in the pore network, which demands a certain degree of hydrophobicity.[6] This is usually achieved by chemical surface modification, consisting in the silylation of the hydroxylated surface of the wet gel pores by an alkylalkoxysilane or an alkylchlorosilane.[2,3,7,8] Yet, although this process may be the answer to a good performance−low cost compromise, it involves undesired environmental risks, namely, the release of hazardous HCl. An alternative approach may be chemical control of the gel's final structure by manipulation of the processing parameters. Among them are the hydrolysis ratio, R (molar ratio H_2O/orthosilicate), the pH, and the solvent nature, whose influences have been thoroughly analyzed for one-step synthesis processes.[2,3]

The purpose of the present work is to report the progress made toward obtaining stable (hydrophobic), low-density (highly porous) TEOS-derived xerogels, by chemical control of the hydrolysis and condensation steps, avoiding harmful surface modification and expensive supercritical solvent extraction. This was achieved by a careful selection of the solvent and by adjusting the catalysts contents in a two-step synthesis process. A brief review on the role of these parameters will follow.

The solvent affects not only the statistical interactions between reacting species but also the surface tension and contact angle upon gel drying; thus, it becomes one of the determining parameters of the xerogel morphology. The capillary pressure, P_c, which usually inhibits

* To whom correspondence should be addressed. E-mail: lilharco@ist.utl.pt.
[†] Centro de Química-Física Molecular.
[‡] ICEMS (Instituto de Ciência e Engenhariade Materiais e Superfícies).

(1) *J. Non-Cryst. Solids* **2001**, *285* (1−3). Proceedings of the Sixth International Symposium on Aerogels, AEROGELS (ISA-6), Albuquerque, NM, 2000.
(2) Yoldas, B. E.; Annen, M. J.; Bostaph, J. *Chem. Mater.* **2000**, *12*, 2475.
(3) Brinker, C. J.; Scherer, S. W. *Sol−Gel Science: The Physics and Chemistry of Sol−Gel Processing*; Academic Press: New York, 1990.
(4) Hæreid, S.; Dahle, M.; Lima, S.; Einarsrud, M. A. *J. Non-Cryst. Solids* **1995**, *186*, 96.
(5) Hæreid, S.; Nilsen, E.; Ranum, V.; Einarsrud, M. A. *J. Sol-Gel Sci. Technol.* **1997**, *8*, 153.
(6) Jeong, A. Y.; Goo, S. M.; Kim, D. P. *J. Sol-Gel Sci. Technol.* **2000**, *19*, 483.
(7) Prakash, S. S.; Brinker, C. J.; Hurd, A. J. *J. Non-Cryst. Solids* **1995**, *190*, 264.
(8) Fidalgo, A.; Rosa, M. E.; Ilharco, L. M., accepted for publication in *Emerging Fields in Sol−Gel Science and Technology*; Lopez, T., Avnir, D., Aegerter, M., Eds.; Kluwer Academic Publishers: New York, 2003.

10.1021/cm031013p CCC: $25.00
Published on Web 04/23/2003

the production of monolithic highly porous silica xerogels at atmospheric pressures, is given by[3]

$$P_c = 2\gamma \cos \theta / r \quad (1)$$

Thus, P_c depends both on the organic medium (through the surface tension, γ, and the contact angle, θ) and on the aged alcogel network (through the average value of the capillary pore radius, r). The capillary pressure may be reduced by decreasing the surface tension or by increasing the liquid wetting angle and/or the pore size.

In the present work the solvent used was 2-propanol, given its recognized ability to yield the highest porosity in silica xerogels prepared by hydrolytic polycondensation of TEOS.[2] For this solvent, the reduction in capillary stress is not related to a low surface tension (it is only slightly lower than those of other common solvents[9]), but to a higher value of θ. Alternatively, 2-propanol can reduce stress during drying by a mechanism similar to that induced by some chemical additives, such as formamide and glycerol:[10] because of its relatively high viscosity,[9] if any residual water were present during drying, the difference in the diffusion coefficients would generate an alcohol gradient, causing a diffusion- rather than a flow-controlled transport mechanism[3].

The initial pH of the precursor solution affects both the rates and the mechanisms of hydrolysis and condensation. Generally, the acid-catalyzed hydrolysis of TEOS (pH ≤ 7, at 25 °C) occurs by a two-step electrophilic mechanism, involving a positively charged transition complex.[11,12] Its rate is controlled by the concentration of H_3O^+ ions in solution, and therefore, the lower the pH, the higher the reaction rate. On the other hand, the hydrolysis rate decreases as the intermediates become more extensively hydrolyzed (as each ethoxide group is replaced by a more electroatractor hydroxyl group). As to the role of the catalyst in the condensation mechanism, two pH domains are usually considered, namely, below and above the isoelectric point of silica (at pH 1.5−2.0).[13−15] Below this point, acid-catalyzed condensation occurs, where the first step is the protonation of a silanol group, followed by condensation preferentially between neutral species and protonated silanols situated in monomers or end groups of chains. It is hindered by extensive hydrolysis or condensation since the positively charged intermediate becomes destabilized. Above the isoelectric point of silica, condensation involves the attack of a nucleophilic deprotonated silanol on a neutral silicate species.[13] The condensation rate is maximized near the neutral pH, where significant concentration of both protonated and deprotonated silanols exist, and is minimized near the isoelectric point.

The two-step process used in the present work allows an efficient separation of the hydrolysis and condensation mechanisms. The first step is carried out in a strong acidic medium, where the condensation reactions are very slow and the hydrolysis proceeds fast (pH ranging from 1.36 to 2.75). Contrasting, the second step takes place at a pH a little above neutrality (achieved by an abrupt addition of NH_3), where hydrolysis is very slow and condensation relatively fast.[15] Thus, when condensation starts, there will be mostly hydroxyl groups bonded to silicon, and some residual unreacted alkoxy groups that will not undergo further hydrolysis. Under these conditions, the base-catalyzed mechanism for condensation may be described by the following equations:[16]

$$(RO)_3Si{-}OH + OH^- \rightarrow (RO)_3SiO^- + H_2O \quad \text{(fast)} \quad (2)$$

$$(RO)_3SiO^- + HO{-}Si(RO)_3 \rightarrow (RO)_3Si{-}O{-}Si(RO)_3 + OH^- \quad \text{(slow)} \quad (3)$$

where R≡H or $Si(OR)_3$. The extent of reaction 2 increases with the silanol's acidity in $(RO)_3Si{-}OH$, which in turn increases as the basicity of the other silicon ligands decreases. This means that the extent of reaction 2 will be greater for polymers in which the Si atoms are more cross-linked via oxygen bridging. Thus, in a solution of polymers with different degrees of cross-linking, the more cross-linked ones will be the most likely to undergo reaction 2 and become available to condensation by reaction 3. The net result is that larger and highly condensed polymers tend to react with feebly acidic monomers to form even more highly condensed species; that is, the larger polymers grow at the expense of the smaller ones, originating a sol of large polymers which, due to extensive cross-linking, are essentially pure silica.[16,17] Since this condensation mechanism is very sensitive to the starting population of condensing species, it is foreseeable to depend also on the hydrolysis catalytic conditions.

The characterization of morphology, structure, porosity, and pore size distribution of the xerogels was made by combining the information from scanning electron microscopy (SEM), envelope density measurements, and nitrogen sorption isotherms. It is shown that when the HCl/TEOS molar ratio for hydrolysis is increased and the NH_3/HCl ratio for condensation is increased up to a certain point, an increase of both pore volume and pore size may be achieved, without a significant decrease in the specific surface area of the xerogels. An important achievement has been the considerable stability of the xerogels toward moisture, which suggests a certain degree of hydrophobicity, even without surface modification.

2. Experimental Section

2.1. Preparation of the Xerogels. The silica wet gels were synthesized by a two-step sol−gel process. The first step consists of the acid-catalyzed hydrolysis of tetraethoxysilane [TEOS, $Si(OC_2H_5)_4$] and the second one of polymerization, by

(9) Lide, D. R. (Editor in Chief) *Handbook of Chemistry and Physics*, 78th Ed.; CRC Press: New York, 1997−1998.
(10) Haranath, D.; Rao, A. V. *J. Porous Mater.* **1999**, *6*, 55.
(11) Aelion, R.; Loebel, A.; Eirich, F. *J. Am. Chem. Soc.* **1950**, *72*, 5705.
(12) Brinker, C. J. *J. Non-Cryst. Solids* **1988**, *100*, 31.
(13) Iler, R. K. *The Chemistry of Silica*; Wiley: New York, 1979.
(14) Corriu, R. J. P.; LeClercq, D.; Vioux, A.; Pauthe, M.; Phalippou, J. In *Ultrastructure Processing of Advanced Ceramics*; Mackenzie, J. D., Ulrich, D. R., Eds.; Wiley: New York, 1988.
(15) Pope, E.; Mackenzie, J. *J. Non-Cryst. Solids* **1987**, *87*, 185.
(16) Brinker, C. J.; Keefer, K. D.; Schaefer, D. W.; Ashley, C. S. *J. Non-Cryst. Solids* **1982**, *48*, 47.
(17) Brinker, C. J.; Keefer, K. D.; Schaefer, D. W.; Assink, R. A.; Kay, B. D.; Ashley, C. S. *J. Non-Cryst. Solids* **1984**, *63*, 45.

Table 1. Gel Times, t_G, for Alcogels with Different Catalyst Amounts[a]

alcogel	*x*	hydrolysis pH	*y*	t_G (min)
$HYD_{0.5}$	0.0005	2.75	1.0	160
HYD_1	0.001	2.45	1.0	54
HYD_3	0.003	1.88	1.0	35
HYD_5	0.005	1.71	1.0	18
HYD_7	0.007	1.54	1.0	8
HYD_9	0.009	1.36	1.0	8
$COND_7$	0.003	1.88	0.7	60
$COND_{10}$	0.003	1.88	1.0	36
$COND_{13}$	0.003	1.88	1.3	27
$COND_{17}$	0.003	1.88	1.7	9

[a] Samples HYD_3 and $COND_{10}$ are equivalent and were prepared for reproducibility check.

condensation of the resulting silanol groups, induced by the addition of ammonia. TEOS (from Alpha Products, 99%) was previously diluted in 2-propanol (i-PrOH, p.a. from Riedel-de Haën), and distilled−deionized water was added, dropwise, under stirring. The reaction mixture was acidified with HCl (p.a. from Merck) and its pH measured, without correction for a nonaqueous medium. The acidic sol was placed in a sealed container, heated at 60 °C, and stirred (at 140 rpm) for 60 min. The required amount of ammonia (NH_3, from Merck, 33%) was then added, and the resulting homogeneous sol was left to gel, with no further stirring. Following this general procedure, two sets of alcogels were prepared with molar compositions TEOS/H_2O/i-PrOH = 1/4/9.2 and different HCl/TEOS (*x*) and NH_3/HCl (*y*) molar ratios, *x* ranging from 0.0005 to 0.009 and *y* from 0.7 to 1.7. They are identified as HYD_{1000x} and $COND_{10y}$. To strengthen the silica network, the alcogels were aged for 48 h at 60 °C: the first 24 h in the residual liquid and the latter in an aging solution containing TEOS, i-PrOH, and H_2O in the same proportions as used for gelation. After measurement of the volume of the aged gels, the pore liquid was exchanged with i-PrOH to completely remove any residual water or TEOS. The washed gels were subcritically dried at 60 °C under ambient pressure, partially covered, until the weight loss became negligible.

2.2. Sample Characterization. The envelope density of the dried gels, outgassed at room temperature prior to weighing, was determined with a GeoPyc 1360, by Micromeritics, using a consolidation force of 50 N for 17 measurement cycles. The measured envelope volume was also used to determine the volume shrinkage of the aged gels upon drying. The structure of the gels was observed using scanning electron microscopy (SEM). Fractured surfaces of the samples were examined with a Hitachi S4100-1, operating at 25 kV. The surfaces were previously sputter-coated with a gold layer ~20-nm thick, to avoid charging effects during observation. The pore structure was studied by N_2 adsorption−desorption isotherms (at 77 K) of the samples, previously outgassed for 24 h at 273 K, using an ASAP 2000 by Micromeritics.

3. Results and Discussion

3.1. Gel Times. In one-step sol−gel processes, the gel times are commonly used as a rough measure of the overall (hydrolysis−condensation) reaction kinetics. In two-step processes, those times may provide more detailed information on the individual reactions. The gel times, t_G, expressed in minutes after the addition of ammonia, are indicated in Table 1 for all the samples, along with the corresponding values of *x* and *y* (HCl/TEOS and NH_3/HCl molar ratios, respectively).

It is clear that the gel times are significantly influenced by the relative amount of acid used in the first step, steeply decreasing with a small decrease in the hydrolysis pH (HYD series), and by the base content in the second step, decreasing as the relative amount of NH_3 added to the same prehydrolyzed mixture increases (COND series).

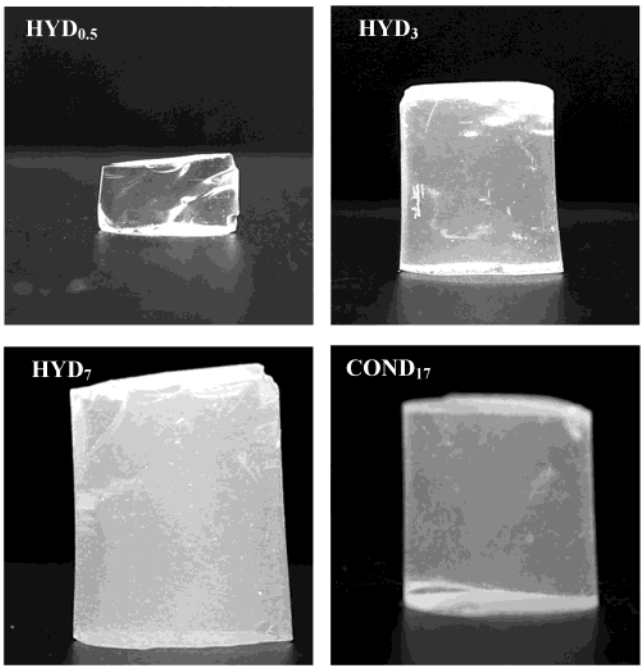

Figure 1. Photographs of selected xerogels, as labeled.

In all the samples of the HYD series, the second step proceeded in similar conditions (close to neutralization), but departing from different populations of condensing species, depending on the extent of hydrolysis until the addition of ammonia. For the lower pH samples, hydrolysis may have been almost complete prior to condensation. In the COND series, in contrast, the first step is similar, and the condensation rates depend on the amount of catalyst. The evolution on the gel times is indicative that gelation is faster for a higher hydrolysis extent in the first step and, when the degree of hydrolysis is the same, for a higher condensation rate in the second step.

3.2. Volume Shrinkage upon Drying, Envelope Density, and Porosity. The gels were rod-shaped, as shown in Figure 1, so that the dimensions of the aged wet gels were easy to evaluate. The shrinkage upon drying (τ_D) may be readily obtained by comparing the aged gels volume (V_a) with the envelope volume (V_e) of the dried and outgassed gels, measured for the envelope density (ρ_e) determination: $\tau_D(\%) = 100 \times (V_a - V_e)/V_a$. The specific pore volume (V_p) and the porosity (P_r) of the xerogels may be calculated from the envelope and skeletal densities (ρ_e and ρ_s), using the relations $V_p = 1/\rho_e - 1/\rho_s$ and $P_r(\%) = 100 \times (1 - \rho_e/\rho_s) = 100 \times V_p/(V_p + 1/\rho_s)$, respectively.[18] In the absence of measured skeletal densities, V_p and P_r were estimated using $\rho_s = 2.1$ g cm^{-3} for all the samples.[19] The results are summarized in Table 2.

When the initial sol volume (22 cm^3 in all samples) is compared with the values of V_a in Table 2, it appears that, under the present preparation procedure, the gel shrinkage upon aging is not so sensitive to the hydrolysis pH as reported by Pajonk et al.[20] On the other hand,

(18) Gregg, S. J.; Sing, K. S. W. *Adsorption, Surface Area and Porosity*, 2nd ed.; Academic Press: London, 1982.
(19) Woignier, T.; Phalippou, J. *J. Non-Cryst. Solids* **1987**, *93*, 17.

Table 2. Catalyst Effect on Volume Shrinkage upon Drying (τ_D), Envelope Density (ρ_e), Total Pore Volume (V_p), and Porosity (P_r) of the Xerogels[a]

sample	V_a (cm^3)	V_e (cm^3)	τ_D (%)	ρ_e (g cm^{-3})	V_p (cm^3 g^{-1})	P_r (%)
$HYD_{0.5}$	20.2 ± 0.1	1.556 ± 0.004	92.3	1.078 ± 0.003	0.451 ± 0.002	48.7 ± 0.3
HYD_1	19.6 ± 0.1	1.86 ± 0.01	90.5	0.900 ± 0.003	0.635 ± 0.004	57.1 ± 0.4
HYD_3	19.3 ± 0.1	2.42 ± 0.01	87.5	0.682 ± 0.002	0.989 ± 0.003	67.5 ± 0.3
HYD_5	18.2 ± 0.1	3.19 ± 0.01	82.5	0.515 ± 0.002	1.47 ± 0.01	75.5 ± 0.4
HYD_7	19.0 ± 0.1	3.929 ± 0.004	79.3	0.4197 ± 0.0003	1.906 ± 0.002	80.0 ± 0.1
HYD_9	19.5 ± 0.1	4.38 ± 0.01	77.5	0.371 ± 0.001	2.219 ± 0.004	82.3 ± 0.2
$COND_7$	19.1 ± 0.1	1.78 ± 0.02	90.7	0.93 ± 0.01	0.59 ± 0.01	65 ± 1
$COND_{10}$	17.9 ± 0.1	2.43 ± 0.01	86.4	0.680 ± 0.002	0.994 ± 0.004	67.6 ± 0.3
$COND_{13}$	18.2 ± 0.1	3.07 ± 0.01	83.1	0.444 ± 0.001	1.775 ± 0.004	78.8 ± 0.2
$COND_{17}$	17.8 ± 0.1	3.04 ± 0.01	82.9	0.521 ± 0.001	1.443 ± 0.003	75.2 ± 0.2

[a] V_a = volume of the aged alcogels; V_e = envelope volume of the outgassed xerogels.

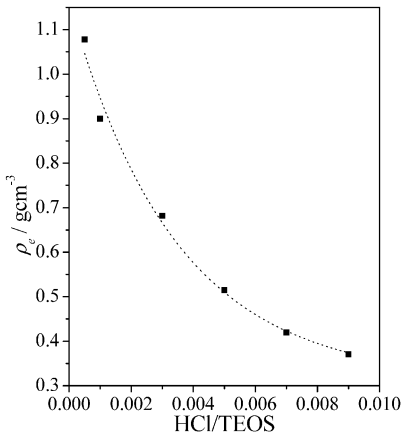

Figure 2. Envelope density (ρ_e) as a function of the molar ratio x (HCl/TEOS).

it is obvious that the hydrolysis pH has a very strong effect on τ_D: the volume shrinkage upon drying can be considerably reduced by a slight increase in the acid catalyst concentration.

The differences in volume shrinkage may be understood in terms of different responses of the structures to the removal of solvent upon drying. During this process, the tension in the liquid is balanced by the compressive stress in the solid network, and the magnitude of the resulting shrinkage depends on its bulk modulus. When it is large enough to withstand the capillary pressure, the critical drying point is attained: the network stops shrinking, and further evaporation causes the menisci to recede into the pores. From this point on, the compressive stress is released and, depending on the alcogel network, the volume shrinkage can be irreversible, or springback can occur.[7] When the hydrolysis extent is increased in the first step (increasing the acid catalyst content), larger and more cross-linked polymers are expected to form according to the proposed condensation mechanism, the silica network becomes stiffer, and the net shrinkage upon drying is reduced.

The shrinkage upon drying is obviously related to the envelope density and percent porosity of the xerogels: there is a drastic decrease in the envelope density from 1.08 to 0.37 g cm^{-3} (corresponding to an increase in porosity from about 49 to 82%) as the hydrolysis pH decreases from 2.75 ($HYD_{0.5}$) to 1.36 (HYD_9). In summary, and as shown in Figure 2, with a slight change in the hydrolysis pH (controlled by the HCl/TEOS molar ratio), the properties of the final product may be varied from a dense xerogel to what can be considered an aerogel.

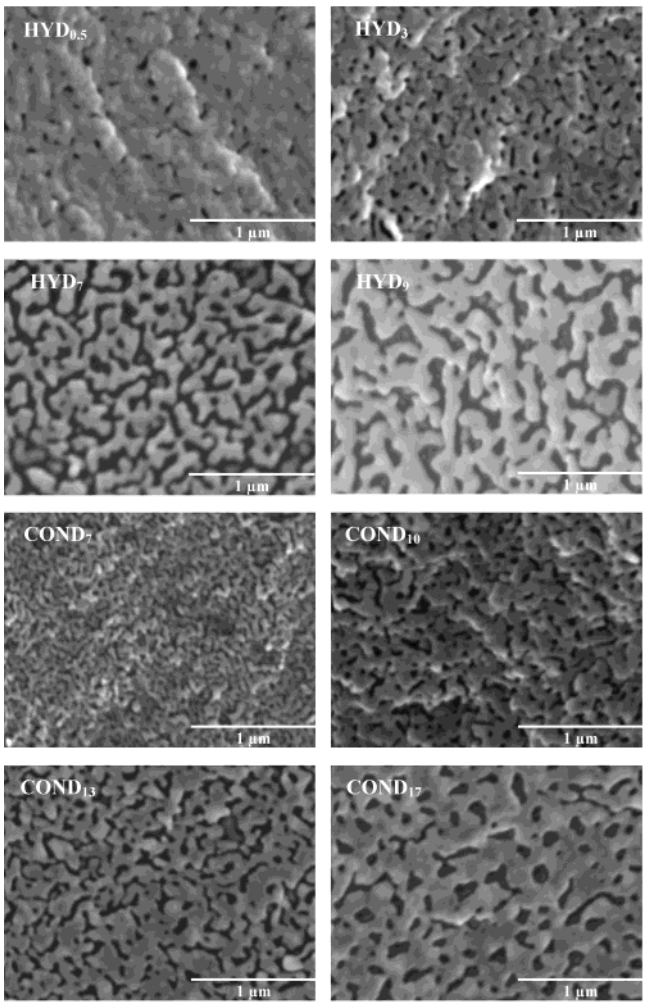

Figure 3. SEM microphotographs of selected xerogels, as labeled.

The relative amount of base used in the second step has a minor effect on the physical properties of the xerogels. This can be seen in Table 2 for the series of xerogels prepared with $x = 0.003$ (identical to sample HYD_3): increasing y from 0.7 to 1.3 causes a decrease in the envelope density, with the corresponding increase in percent porosity from 65 to 79%; a further increase in that ratio reflects a small increase in the envelope density. This trend points to the existence of an opti-

(20) Pajonk, G. M.; Elaloui, E.; Achard, P.; Chevalier, B.; Chevalier, J. L.; Duran, M. *J. Non-Cryst. Solids* **1995**, *186*, 1.

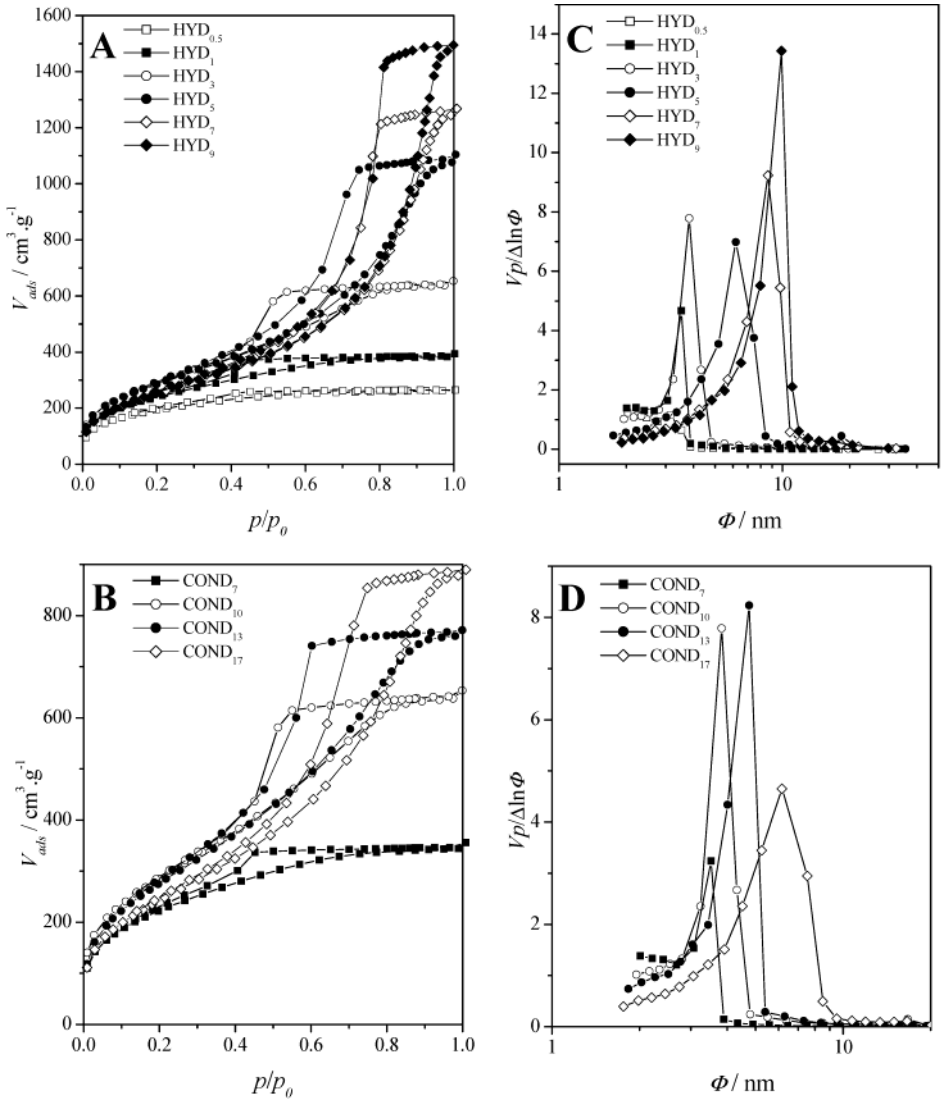

Figure 4. N_2 adsorption−desorption isotherms of samples prepared with different hydrolysis (A) and condensation (B) catalytic conditions. Corresponding BJH pore size distributions (C and D).

mum molar ratio of NH_3/HCl that must correspond to neutralization of the acidic sol, although the gelation pH was not measured. Below that ratio, the condensation is slow enough to allow hydrolysis to proceed simultaneously. The global reaction mechanism thus behaves more similarly to a one-step process, resulting in a more compact structure, as would be expected for such low hydrolysis pH values.[16,17] A remark is deserved to the good reproducibility of results between samples HYD_3 and $COND_{10}$.

3.3. Particle Morphology. With the exception of samples $HYD_{0.5}$ and $COND_7$, which were transparent, the xerogels were translucent (see Figure 1), certainly due to light scattering by the aggregate structure of these materials. A closer inspection by SEM revealed different surface morphologies, ranging from granular to highly porous interconnected macroporous structures,[10] where both the silica skeleton and the macropores are continuous. The SEM microphotographs of samples $HYD_{0.5}$, HYD_3, HYD_7, HYD_9, $COND_7$, $COND_{10}$, $COND_{13}$, and $COND_{17}$ are shown in Figure 3.

A morphology change from granular to bicontinuous is clearly seen when comparing sample $HYD_{0.5}$ with all the others. Additionally, with decreasing hydrolysis pH (increasing ratio x) there is a consistent increase in the particle and macropore sizes. The same type of morphological evolution is observed with increasing y (molar ratio NH_3/HCl), although in this case the granular structure was not observed. This is not surprising, given that all the COND samples were prepared with a hydrolysis pH equivalent to HYD_3. The resemblance of samples HYD_3 and $COND_3$ is evident.

The SEM observations are consistent with the calculated volume shrinkage upon drying. As stated above, increasing the hydrolysis extent induces the formation of larger and more cross-linked polymers, resulting in a more or less randomly packed array of interconnected identifiable particles surrounded by large voids (the macropores). These voids, associated with the less deformable nature of the silica polymers, may account for the observed springback in the corresponding samples since they help to prevent further condensation during drying. When the hydrolysis extent is insufficient ($HYD_{0.5}$), the strong surface tensions generated by removal of the solvent cause the polymers to deform and impinge one another, promoting the formation of more cross-links. The overall result is a denser dry gel, with a granular morphology and without macropores.

Table 3. BET Parameters, Surface Area (S_{BET}), Total Pore Volume (V_p), and Pore Diameter (Φ) Calculated for All the Xerogels[a]

	BET parameters				
sample	c	$V_{m,STP}$ ($cm^3\ g^{-1}$)	S_{BET} ($m^2\ g^{-1}$)	V_p ($cm^3\ g^{-1}$)	Φ (nm)
$HYD_{0.5}$	140 ± 43	157 ± 2	685 ± 10	0.41	2.39 ± 0.04
HYD_1	87 ± 6	199 ± 1	866 ± 5	0.61	2.82 ± 0.02
HYD_3	68 ± 4	240 ± 1	1046 ± 6	1.01	3.86 ± 0.02
HYD_5	66 ± 4	242 ± 2	1053 ± 6	1.66	6.32 ± 0.04
HYD_7	56 ± 3	215 ± 1	936 ± 5	1.92	8.23 ± 0.04
HYD_9	58 ± 3	217 ± 1	944 ± 5	2.31	9.79 ± 0.05
$COND_7$	91 ± 12	185 ± 2	805 ± 8	0.53	2.65 ± 0.03
$COND_{10}$	68 ± 4	240 ± 1	1046 ± 6	1.01	3.86 ± 0.02
$COND_{13}$	50 ± 1	238 ± 1	1035 ± 4	1.69	4.61 ± 0.02
$COND_{17}$	56 ± 1	208 ± 1	904 ± 3	1.36	6.01 ± 0.02

[a] BET equation: $(V/V_m) = (cx)/\{(1 - x)[1 + (c - 1)x]\}$, with $x = p/p_0$.

3.4. Pore Morphology. Figure 4 includes the nitrogen adsorption−desorption isotherms of the samples HYD (Figure 4A) and COND (Figure 4B). The corresponding pore size distributions (PSDs), calculated from the desorption isotherms using the Barrett−Joyner−Halenda (BJH) algorithm,[21] assuming a cylindrical pore shape, are presented in Figure 4C,D.

All the adsorption−desorption isotherms are type IV and show the hysteresis loops usually associated with capillary condensation in mesopores.[22,23] The macroporous structures observed by SEM are too large to be observed by N_2 sorption analysis (>50 nm). Thus, these xerogels show a hierarchical pore structure, similar to the one obtained by Takahashi et al. by spinodal decomposition of poly(ethylene oxide)-doped silica.[24] This bimodal pore structure contains mesopores within the individual particles and macropores that are the interstitial voids between them.

From Figure 4C,D, it is evident that the pore size distribution shifts to higher diameters with increasing ratios x and y. A Brunauer−Emmett−Teller (BET) analysis[25] of the amount of N_2 gas adsorbed at various partial pressures, p/p_0 (at least five points, $0.05 < p/p_0 < 0.3$, using a nitrogen cross-sectional area of 16.2 Å^2), was used to find the specific surface area, S_{BET}, and a single condensation point (at $p/p_0 = 0.99$) was used to estimate the total pore volume (V_p). The average pore diameter for cylindrical pores (Φ) was calculated from these values of V_p ($\Phi = 4V_p/S_{BET}$), with the caution associated with a unique point value. The results are summarized in Table 3.

The values of parameter c lie within the range of applicability of the BET isotherm, and by not being too high, they indicate that the samples are not microporous. All the samples present large surface areas, S_{BET}. The absolute values of V_p are generally in good agreement with those in Table 2. The variations in V_p are determined by the ratios x and y, accompanying the envelope density results: the total pore volume increases with increasing x, and with increasing y up to a certain point. The evolution of the average pore size (Φ) with x conforms to that of V_p, whereas S_{BET} presents a maximum for HYD_5. This suggests a change in the mesopore morphology, from a network of undefined shapes to a network of open-ended cylinders.[8] Such is consistent with the observable change in the hysteresis loops of the N_2 isotherms when going from sample HYD_3 to HYD_7 (Figure 4A), from type H2 (characteristic of corpuscular systems) to H1 (characteristic of capillary condensation and desorption in open-ended cylindrical pores).[18,23,26] Similar conclusions may be inferred from Figure 4B when going from sample $COND_{10}$ to $COND_{17}$.

Table 4. Cumulative Desorption Pore Volume (V_{BJH}), Pore Diameter (Φ_{BJH}) and Porosity Percentage (P_{RBJH}) Calculated for All the Xerogels

sample	V_{BJH} ($cm^3\ g^{-1}$)	Φ_{BJH} (nm)	P_{rBJH} (%)
$HYD_{0.5}$	0.31	1.81	39
HYD_1	0.57	2.63	54
HYD_3	1.07	4.09	69
HYD_5	1.72	6.54	78
HYD_7	1.95	8.35	80
HYD_9	2.31	9.82	83
$COND_7$	0.49	2.44	51
$COND_{10}$	1.07	4.09	69
$COND_{13}$	1.24	4.81	72
$COND_{17}$	1.41	6.22	75

Another approach to the average pore size was obtained from the BJH analysis, using the cumulative desorption pore volume in the mesopore range (V_{BJH}).[18] These volumes were also used to calculate the porosity percentage (P_{rBJH}), taking $\rho_s = 2.1\ g\ cm^{-3}$, as above. The results are summarized in Table 4.

The V_{BJH} values are generally in good agreement with the V_p values obtained from the envelope densities (Table 2) and from the adsorption single condensation point (Table 3), except for the less porous samples ($P_r < 70\%$). This discrepancy can be explained by the existence of a pore-blocking effect during desorption that yields lower P_r values in those samples.[18] There is also a good agreement between porosity and pore diameters determined by the different methods.

4. Conclusions

The chemical control through pH manipulation in a two-step sol−gel process allowed the production of monolithic silica xerogels, with low density and high surface area, in all similar to aerogels. They are cellular materials with a bimodal pore distribution, built upon a uniform array of twisted, interconnected particles and macropores, containing a narrow mesopore size distribution within the solid network. These low-density xerogels are extremely stable under atmospheric conditions, suggesting that they must have some degree of hydrophobicity. A structural analysis is needed to highlight the chemical and structural modifications imparted by the catalytic conditioning, responsible for such physical properties. Particularly, the proportion of residual silanol groups in the silica network and possible changes

(21) Barrett, E. P.; Joyner, L. G.; Halenda, P. P. *J. Am. Chem. Soc.* **1951**, *73*, 373.
(22) Barton, T. J.; Bull, L. M.; Klemperer, W. G.; Loy, D. A.; McEnaney, B.; Misono, M.; Monson, P. A.; Pez, G.; Scherer, G. W.; Vartuli, J. C.; Yaghi, O. M. *Chem. Mater.* **1999**, *11*, 2633.
(23) Sing, K. S. W.; Everett, D. H.; Haul, R. A. W.; Moscou, L.; Pierotti, R. A.; Rouquérol, J.; Siemieniewska, T. *Pure Appl. Chem.* **1985**, *57*, 603.
(24) Nakamura, N.; Takahashi, R.; Sato, S.; Sodesawa, T.; Yoshida, S. *Phys. Chem. Chem. Phys.* **2000**, *2*, 4983.
(25) Brunauer, S.; Emmett, P. H.; Teller, E. *J. Am. Chem. Soc.* **1938**, *60*, 309.
(26) Ravikovitch, P. I.; Neimark, A. V. *J. Phys. Chem. B* **2001**, *105*, 6817.

in the siloxane backbone structural arrangement are relevant. A work in preparation will focus on this matter.

Acknowledgment. This work was funded by Fundação para a Ciência e Tecnologia (FCT)−Project POCTI/CTM/33487/2000. The authors wish to thank Prof. Rui Almeida (INESC) for kindly granting accessibility to the ASAP 2000. A. Fidalgo is grateful to FCT for Ph.D. Grant PRAXIS XXI/BD/19815/99.

CM031013P